Revista Mexicana de Astronomía y Astrofísica, **00**, ??–?? (2007)

arXiv:1609.02201v1 [astro-ph.SR] 7 Sep 2016

CHEMICAL ABUNDANCES FOR A-AND F-TYPE SUPERGIANT STARS

R. E. Molina,[1] and H. Rivera,[1]

Received ; accepted

RESUMEN

Hemos efectuado un análisis detallado de las abundancias químicas de cuatro objetos supergigantes HD 45674, HD 180028, HD 194951 y HD 224893, usando espectros de alta resolución ($R \sim 42{,}000$) tomados de la libreria ELODIE. Se presentan los primeros resultados de las abundancias para HD 45674 y HD 224893, y se reafirman las abundancias para HD 180028 y HD 194951 calculadas por Luck (2014). Los elementos alfa nos indican que todos los objetos estudiados pertenecen a la población del disco galáctico. A partir de sus abundancias y de su localización en el diagrama Hertzsprung-Russell parece indicarnos que HD 45675, HD 194951 y HD 224893 evolutivamente se encuentran en la fase posterior al primer dragado (post-1DUP) y se mueven en la región del red-blue loop. HD 180028 muestra abundancias típicas de la población I pero su estado evolutivo no puede ser definido satisfactoriamente.

ABSTRACT

We present the stellar parameters and elemental abundances of a set of A–F-type supergiant stars HD 45674, HD 180028, HD 194951 and HD 224893 using high resolution ($R \sim 42{,}000$) spectra taken from ELODIE library. We present the first results of the abundance analysis for HD 45674 and HD 224893. We reaffirm the abundances for HD 180028 and HD 194951 studied previously by Luck (2014) respectively. Alpha-elements indicates that objects belong to the thin disc population. From their abundances and its location on the Hertzsprung-Russell diagram seems point out that HD 45675, HD 194951 and HD 224893 are in the post-first dredge-up (post-1DUP) phase and they are moving in the red-blue loop region. HD 180028, on the contary, shows typical abundances of the population I but its evolutionary status could not be satisfactorily defined.

Key Words: Stars: atmospheric parameters — Stars: abundances — Stars: evolution — Stars: supergiant

1. INTRODUCTION

The process of chemical evolution in the Galaxy can be understood from its massive stars. These objects in their rapid evolution undergo changes through the process of nucleosynthesis over time and return their chemical elements into the interstellar medium from stellar winds and supernova events. It is not surprise the existence of massive young objects in the galactic plane since it is an area of star formation. These objects are visually luminous in galaxies and, in general, suitable candidates for studies of stellar and chemical evolution (Luck et al. 1998; Smiljanic et al. 2006; Venn et al. 2000, 2001, 2003; Kaufer et al. 2004).

In the galactic disc, some of these massive objects have been classified as supergiant stars with masses between 5 to 20 $M_\odot$, with A-and-F spectral type, which are moderately evolved and where the chemical abundances of the light elements CNO have been key to discriminate their evolutionary states (Lyubimkov et al. 2011, Venn 1995a,1995b and internal references). For massive stars when H is exhausted, the post-He core burning phase can be affected in several ways.

Stellar evolutionary models constructed at solar metallicities predict that massive supergiants ($M \geq 10\,M_\odot$) are in the phase of helium core burning (Schaller et al. 1992; Stothers & Chin 1991). These objects have already left the main sequence on the

[1]Laboratorio de Investigación en Física Aplicada y Computacional, Universidad Nacional Experimental del Táchira, CP 5001, Venezuela.

Hertzsprung-Russell diagram (HRD) and begins the ignition of He in the blue supergiant region but thermal instabilities causes in the star a rapid expansion towards the red supergiant one. In this last phase, the A–F supergiants are able to resume thermal and radiative equilibrium through convection in the outer layers and shows an altered CNO abundances due to the first dredge-up (1DUP) event.

On the other hand, A–F supergiants less massive ($M < 10\,M_{\odot}$) have also initiated the He-core burning without visiting the red giant branch, a fully convective intermediate zone is predicted, the envelope is able to establish the thermal equilibrium and the stars are kept in the blue supergiant phase. Under these conditions CNO abundances remain unchanged (Stothers & Chin 1976; 1991).

However, another scenario is possible for objects with intermediate masses ($3 < M < 9\,M_{\odot}$) and is called the blue loop. In this point the star has eventually developed a convective envelope and is rising up the Hayashi line in the HRD. These objects have already reached the red supergiant stage but eventually evolved back into a blue supergiant phase (Walmswell et al. 2015). During the red supergiant phase, the convective zone mixing materials of H-burning shell which are subsequently released to the surface by the event of the 1DUP and it show changes in the observed CNO abundance patterns. The amount CNO-processed material in such objects allows to discriminate different types of supergiants.

The main goal of this work is based on a detailed study of chemical abundances for a set of four low-latitude A–F supergiants HD 45674, HD 180028, HD 194951 and HD 224893 under LTE assumption and the determination of their atmospheric parameters from excitation and ionization equilibrium. For this purpose we employ high-resolution spectroscopy and a set of atmospheric models constructed with plane-parallel geometry, hydrostatic equilibrium, local thermodynamic equilibrium (LTE) and the `ODFNEW` opacity distribution (Castelli & Kurucz 2004). It is expected that the abundances derived correspond to the typical abundances observed for supergiant stars in the galactic disc.

This paper are organized as follows: In § 2 regards to the description of the sample selection. In § 3 presents how the atmospheric parameters were estimated. We determine the chemical abundances for the three stars in § 4. An individual analysis of abundances for each stars is present in § 5. In § 6 is dedicated to discuss our results, and finally, in § 7 gives the conclusions of the paper.

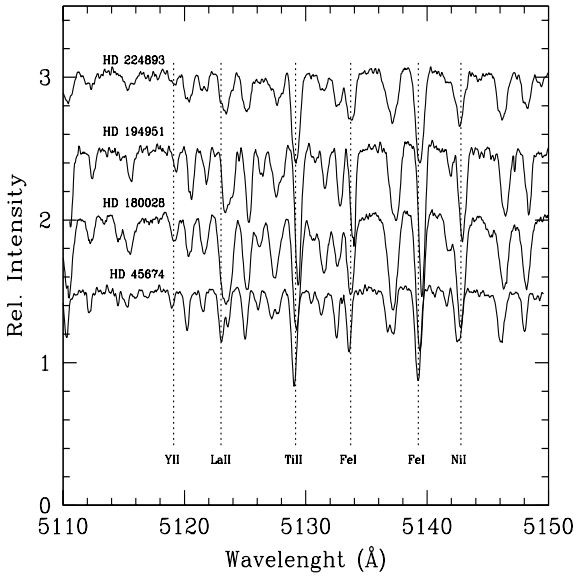

Fig. 1. Representative spectra of the sample stars HD 45674, HD 180028, HD 194951 and HD 224893. The location of lines of certain important elements have been indicated by dashed lines. This stars are arranged in decreasing order the HD number.

2. OBSERVATIONS

2.1. *Sample selection*

The stars for this analysis (HD 45674, HD 180028, HD 194951 and HD 224893) were selected for luminous objects with classes I and II located in the galactic plane. The derived abundances are compared with the mean abundances obtained for a sample of G–K young supergiants of Population I taken from Luck (1977; 1978).

The stellar spectra taken for HD 45674, HD 180028, HD 194951 and HD 224893 stars come from the library ELODIE[2] originally published by Moultaka et al. (2001) and updated in its version 3.1 by Prugniel et al. (2007). The spectra were observed on July 06, 1999; on July 26, 2003; on December 18, 1999 and on July 07, 1999 respectively by means of the echelle spectrograph ELODIE placed in the 1.93m telescope located in the Haute-Provence Observatory (OHP). They cover the spectral region between 4000 and 6800 Å,and have a resolving power of $R \approx 42{,}000$. The signal-to-noise ratio (S/N) for HD 45674, HD 180028, HD 194951 and HD 224893 is reported to be 83, 175, 82 and 145 respectively. This S/N per pixel has been derived for all spectra in the library at 5550 Å.

HD 45674, HD 180028 and HD 194951 are objects labeled as IRAS point source, i.e., IRAS 06262 - 0032,

[2] http://atlas.obs-hp.fr/elodie/

TABLE 1

BASIC PARAMETERS FOR THE SAMPLE.

No. HD	SpT	α	δ	V	B	l	b	V_r	π	$E(B-V)$	$v\ sini$
		(h m s)	(^{o} ′ ″)	(mag)	(mag)	(^{o})	(^{o})	(km s^{-1})	(mas)	(mag)	(km s^{-1})
45674	F1Ia	06 28 47	−00 34 20	6.56	7.30	210.85	−05.30	+18.4±0.9	1.31±0.51	0.382	...
180028	F6Ib	19 14 44	+06 02 54	6.96	7.73	040.97	−02.39	−5.1±0.7	-0.32±0.51	0.346	23.3
194951	F1II	20 27 07	+34 19 44	6.41	6.84	073.86	−02.34	−13.5±2.0	1.00±0.41	0.230	20
224893	A8II	00 01 37	+61 13 22	5.57	5.94	116.97	−01.07	−23.2±2.0	1.06±0.27	0.244	40

IRAS 19122 + 0557 and IRAS 20252 + 3410 respectively, although none of them display realiable infrared excesses since their IRAS fluxes evidence a low quality (Q=1) in 25, 60 and 100 microns. A review of the spectral energy distributions (SED) represented from the available photometry using VisieR database, also indicate that fluxes coming from other sources like WISE and AKARI for these three objects does not display infrared excesses. Likewise, HD 224893 does not show evidence of dust around the central star. This last object was identified by Bidelman (1993) as possible candidates to post-AGB or normal A-and F-type supergiant stars.

Figure 1 shows a representative range of 50 Å of the spectrum for the stars HD 45674, HD 180028, HD 194951 and HD 224893. The vertical dotted lines represent the position of some absorption lines of elements such as Y II, La II, Ti II, Fe I y Ni I in this spectral region. The basic parameters for the total sample are in Table 1. This table contains the HD number, the equatorial coordinates, the apparent V and B magnitude, the galactic coordinates, the radial velocity, the parallax, the colour excess and the velocity of rotation. These values were taken from the SIMBAD astronomical database.[3]

3. ATMOSPHERIC PARAMETERS

In order to obtain the atmospheric parameters are necessary accurate measurements of the equivalent widths (EWs) of the Fe lines and also measurements of atomic data ($\log g$ and χ (eV)). The atomic data for Fe I and Fe II lines were taken from Führ & Wiese (2006) and Meléndez & Barbuy (2009). The EWs values were restricted to range from 10 to 200 mÅ, and only non-blended lines were measured. To measure the EWs we used the task `SPLOT` of the `IRAF` software using a Gaussian fit to the observed line profiles. The error in the measurements of EWs is about 8-10%.

The stellar atmospheric models for the abundance determinations were selected from the collection done by Castelli and Kurucz (2003). These models have been constructed with a plane-parallel geometry, hydrostatic equilibrium, local thermodynamic equilibrium (LTE) and the `ODFNEW` opacity distribution.

[3]http://simbad.u-strasbg.fr/simbad/

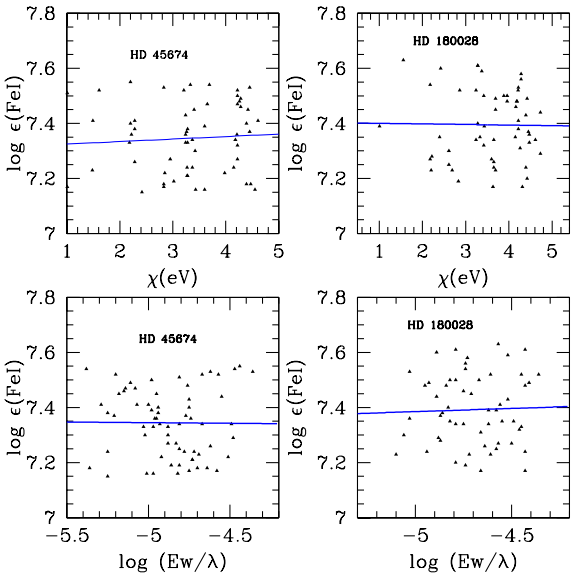

Fig. 2. Independence of Fe I abundances from the low potential excitation and reduced equivalent widths in HD 45674 and HD 180028.

We used the updated version 2010 of the `MOOG` code (Sneden 1973) in the determination of the atmospheric parameters. This code has been developed under ETL assumptions. Based on trial and error test, we selected the model that best fits the photosphere of stars. With the best model, the effective temperature was determined under the assumption of excitation equilibrium, i.e., by requiring that the derived iron abundances should be independent of the low excitation potential. The surface gravity is derived by requesting that the Fe I abundances be similar to those obtained for the Fe II. To confirm the value of gravity, the equilibrium condition can be extended to other elements with two ionization states like Ca, Ti, Cr, Ni. Finally the microturbulence velocity is determined by imposing that the abundances of Fe I are independent of reduced equivalent widths ($\log$ Ew/λ). Figure 2 shows the independence between the abundances of Fe I con-

TABLE 2

ATMOSPHERIC PARAMETERS DERIVED IN THIS WORK AND THOSE OBTAINED FROM LITERATURE.

No HD	T_{eff} (K)	$\log g$	ξ_t (km s^{-1})	[Fe/H]	Ref.
	7346	1.95		+0.18	Prugniel & Soubiran (2001)
45674	7630	2.05		+0.16	Wu et al. (2011)
	7488±200	2.00±0.07		+0.17±0.01	mean value
	7500	2.0	4.0	+0.16	this work (adopted)
	6280	1.72	4.6	−0.03	Gray et al. (2001b)
	6531	1.54		−0.01	Prugniel & Soubiran (2001)
	6050	1.3	3.0		Andrievsky et al. (2002)
180028	6287	1.65		+0.14	Wu et al. (2011)
	6307	1.9	4.0	+0.10	Kovtyukh et al. (2012)
	6488	2.32	4.08	+0.26	Luck (2014)
	6502	2.46	4.11	+0.39	Luck (2014)
	6349±171	1.84±0.42	3.96±0.59	+0.14±0.16	mean value
	6400	2.1	4.8	−0.06	this work (adopted)
	6950	2.02		−0.09	Gray et al. (2001b)
	6350	1.0	2.8		Andrievsky et al. (2002)
194951	7392				Kovtyukh et al. (2007)
	7268				Hohle et al. (2010)
	6760	1.92		−0.13	Lyubimkov et al. (2011)
	7019	2.22	3.93	+0.08	Luck (2014)
	6977	2.21	3.87	+0.11	Luck (2014)
	6959±341	1.87±0.50	3.53±0.64	−0.01±0.12	mean value
	7000	1.8	4.7	−0.15	this work (adopted)
224893	7340	1.96	3.9	−0.24	Gray et al. (2001b)
	7500	2.0	4.5	−0.26	this work (adopted)

cerning to the low potential excitation and reduced equivalent widths for HD 45674 and HD 180028.

From Table 2 can be identified the atmospheric parameters estimated by different authors from photometric and spectroscopic techniques and also the atmospheric parameters adopted from this work. For each object with more than one measures it was estimated a mean value in their atmospheric parameters. We note that our adopted atmospheric parameters match satisfactorily with these mean values.

3.1. *Uncertainty in the abundances*

We calculate the effects on chemical abundances due to errors in the measured equivalent widths (8–10%), the defined model of atmospheric parameters (+250 K in T_{eff}, +0.5 in $\log g$ and +0.5 km s^{-1} in ξ_t), and the atomic data ($\log gf$ and χ (eV)). Errors due to equivalent widths are random because they depend on several factors such as the position of the continuum, the signal to noise ratio (S/N) and the spectral type of the star.

In contrast errors due to the atmospheric parameters and atomic data are systematic and depend on the quality with which they were derived. In short, the error in the gf-values can varies from element to element. For example, experimental values of high accuracy for Fe I and Fe II between 3% to 10% are available for a large fraction of lines. For other Fe-peak elements, errors in their gf-values may range from 10 to 25%. For neutron- capture elements the accuracy is the 10 to 50% range. The sensitivity of derived abundances to changes in the model atmosphere parameters are described in Table 3.

HD 45674 and HD 194951 have the same temperature, i.e., 7500 K. For these stars the spectra are much cleaner and the temperature are not large enough for the lines to develop strong wings making line strengths inaccurate. We can see that a variation in effective temperature of 250 K generates greater uncertainty in all lines, particularly in neutral lines except C, N, O and ionized lines like Ba, Ce and Nd. Contrary we did not observe significant changes in the uncertainties due to changes in $\log g$ by 0.5, ξ_t by 0.5 km s^{-1} and Ew by 10 per cent. On the other hand, a lower temperature (6400 K) the line strenghts shows sensitivity only to changes either in T_{eff} by 250 K and $\log g$ by 0.5.

The total error σ_{tot} for each element is given by the square root of the quadratic sum of the random and systematic errors.

4. DETERMINATION OF THE ABUNDANCES

In the determination of chemical abundances we use the equivalent widths of 176, 116, 184 and 73 absorption lines identified in HD 45674, HD 180028, HD 194951 and HD 224893 respectively. For this

TABLE 3

SENSITIVITY OF ABUNDANCES TO THE INCERTAINTIES IN THE MODEL PARAMETERS FOR TWO RANGE OF TEMPERATURE COVERING OUR SAMPLE STARS.

	HD 45674 (7500 K)					HD 180028 (6400 K)				
Species	ΔT_{eff} +250 K	$\Delta \log g$ +0.5	$\Delta \xi_t$ +0.5	ΔEw +10%	σ_{tot}	ΔT_{eff} +250 K	$\Delta \log g$ +0.5	$\Delta \xi_t$ +0.5	ΔEw +10%	σ_{tot}
C I	−0.14	0.00	+0.01	−0.01	0.14	+0.07	−0.11	−0.01	0.00	0.13
N I	−0.02	−0.06	0.00	−0.01	0.06	···	···	···	···	···
O I	+0.02	−0.08	+0.01	−0.01	0.08	+0.10	−0.05	0.00	···	0.11
Na I	−0.20	+0.08	+0.01	−0.01	0.22	−0.03	−0.03	+0.05	−0.01	0.07
Mg I	−0.22	+0.08	+0.08	−0.01	0.25	−0.14	−0.04	+0.04	0.00	0.15
Si I	···	···	···	···	···	−0.03	−0.03	+0.01	0.00	0.04
Si II	+0.02	−0.08	+0.16	−0.02	0.18	+0.13	−0.15	+0.07	−0.01	0.21
S I	−0.17	+0.04	+0.02	−0.01	0.18	+0.04	−0.11	+0.02	−0.01	0.12
Ca I	−0.27	+0.10	+0.05	−0.01	0.29	−0.07	−0.02	+0.04	−0.01	0.08
Ca II	−0.07	−0.04	+0.03	0.00	0.09	···	···	···	···	···
Sc II	−0.15	−0.12	+0.07	−0.01	0.20	−0.04	−0.16	+0.03	−0.01	0.17
Ti I	−0.28	+0.05	0.00	−0.02	0.29	−0.14	−0.04	+0.01	−0.01	0.15
Ti II	−0.15	−0.13	+0.08	−0.02	0.21	−0.03	−0.16	+0.04	−0.01	0.17
V II	−0.13	−0.12	+0.02	−0.01	0.18	···	···	···	···	···
Cr I	−0.27	+0.06	+0.03	−0.01	0.28	−0.12	−0.04	+0.03	−0.01	0.13
Cr II	−0.10	−0.12	+0.05	−0.01	0.16	+0.03	−0.16	+0.06	−0.02	0.17
Mn I	−0.24	+0.07	+0.02	−0.01	0.25	−0.08	−0.04	+0.04	−0.01	0.10
Fe I	−0.24	+0.07	+0.03	−0.01	0.25	−0.08	−0.04	+0.04	−0.01	0.10
Fe II	−0.10	−0.12	+0.04	−0.01	0.16	+0.02	−0.15	+0.05	−0.01	0.16
Ni I	−0.22	+0.08	+0.01	0.00	0.23	−0.08	−0.04	+0.02	−0.01	0.09
Cu I	···	···	···	···	···	−0.13	−0.04	+0.01	−0.01	0.14
Zn I	−0.24	+0.07	+0.01	0.00	0.25	−0.08	−0.05	+0.02	−0.01	0.10
Y II	−0.19	−0.11	+0.03	−0.01	0.22	−0.04	−0.16	+0.02	0.00	0.17
Zr II	−0.17	−0.13	+0.05	−0.02	0.22	−0.03	−0.16	+0.01	0.00	0.16
Ba II	−0.30	0.00	+0.05	−0.01	0.30	−0.10	−0.10	+0.07	···	0.15
La II	···	···	···	···	···	−0.08	−0.16	+0.06	−0.02	0.19
Ce II	−0.24	−0.08	+0.01	−0.01	0.25	−0.08	−0.15	+0.01	0.00	0.17
Nd II	−0.28	−0.05	0.00	0.00	0.28	−0.11	−0.15	+0.01	0.00	0.19
Eu II	···	···	···	···	···	−0.10	−0.18	0.00	···	0.20

purpose we use the task ABFIND of the MOOG code (Sneden 1973). We employ the atmospheric models adopted in Table 2. The sources of the gf-values for different elements are those that have been referred by Sumangala Rao, Giridhar and Lambert (2012) (see Table 4 for further details).

Sumangala Rao, Giridhar and Lambert (2012) also studied the systematic differences caused when they made use different sources for gf-values. The authors employed for this purpose the solar spectrum taken from Solar Flux Atlas (Kurucz et al. 1984) and found very few differences to solar values for most of the elements, i.e., between 0.04 to 0.09 dex.

The chemical abundances derived for HD 45674, HD 180028, HD 194951 and HD 224893 can be seen in Table 4. This table contains the chemical species present in the photosphere, the solar photospheric abundances are given by Asplund et al. (2005), as well as those calculated for each stars and its uncertainty, the abundances relative to hydrogen, the number of identified lines and the abundances relative to iron. The abundances of the elements in Table 4 are in a logarithmic scale with respect to hydrogen, namely: $\log \epsilon(\mathrm{X}) = \log [\mathrm{N(X)/N(H)}] + 12.0$. The abundances of the elements relative to hydrogen and iron are expressed as [X/H] = log ϵ(X)star - log ϵ(X)sun and [X/Fe] = [X/H] - [Fe/H] respectively.

5. INDIVIDUAL DISCUSSION OF THE ABUNDANCES

5.1. *HD 45674*

The star HD 45674 has been classified as F1Ia. Bidelman (1993) includes this object as a possible candidate to post-AGB or A-and-F normal supergiant stars. Their atmospheric parameters were obtained from ionization equilibrium between the lines of Fe I and Fe II reaching values of $\mathrm{T_{eff}} = 7500$ K, $\log g = 2.0$, $\chi_{\mathrm{t}} = 4.0$ and [Fe/H] = +0.16 dex respectively. The surface gravity for HD 45674 was reaffirmed from the equilibrium ionization of other elements such as Ca, Ti, Cr, namely $\Delta = [\mathrm{X_{II}/H}] - [\mathrm{X_{I}/H}]$ is 0.08, −0.02 and −0.05 respectively. A recopilation of the atmospheric parameters obtained by different authors are shown in Table 2.

With respect to the abundances of the light elements CNO, the carbon abundance is obtained from two lines (4769 Å and 5380 Å) being their values [C/H] = −0.20 and [C/Fe] = −0.36. Venn (1995b) predicts a non-LTE correction of −0.25 in the C abundance for the supergiant HD 36673 (F0Ib) with effective temperature of 7400 K. HD 45674 has an effective temperature of 7500 K therefore none non-LTE correction must be made. Taking a value of −0.25 dex leads to an abundance of [C/Fe] = −0.69.

The N abundance for HD 45674 shows a moderate enrichement ([N/Fe] = +0.68), in fact this abundance is obtained from λ4151.4 Å line with a EW of 10.1 mÅ. A non-LTE correction of −0.28 is derived by Venn (1995b) in the near IR region at 7400 K for HD 196379 with A9II type. The non-LTE correction made for N I by Luck & Lambert (1985) indicates that at the temperature of 7500 K, an equivalent width of ∼10 mÅ and $\log g =$ 2.0 its value is almost zero (see Figure 8). By contrast, for the blue region Przybilla & Butler (2001) found a non-LTE correction of −0.11 dex for N I (λ3830 Å) at a temperature of 9600 K and where its value increases negatively toward the IR lines. Taking into consideration the above we can argue that the non-LTE correction should be small for this line.

We adopted a value of ∼−0.08 dex for our line in the blue region. Our non-LTE values are [N/H] = +0.60 dex and [N/Fe] = +0.36 dex respectively. The observed deficiency in C and the moderate enhancement in N involves a conversion of initial carbon into N through CN-cycle and products of the 1DUP are brought to the surface.

The O abundance is near to solar value ([O/Fe] = +0.03) and is obtained from λ6156.0 Å and λ6156.8 Å lines. To this temperature a non-LTE correction about of −0.15 taken from Takeda & Takada-Hidai (1998) would lead to abundances of [O/H] = −0.12 and [O/Fe] = −0.36 respectively. The C/O ratio of 0.32 indicates that HD 45674 is O-rich.

Iron-peak elements (Sc, V, Cr, Ni) shows [X/Fe] abundances nearest to solar and ranges from −0.22 to +0.18 dex. The [α/Fe] ratio ∼+0.10±0.16 estimated from Mg, Si, Ca, Ti shows a typical value for objects of thin disk (see Reddy et al. 2003; 2006). Si and S abundances are moderate enhancements, i.e., [Si/Fe] = +0.31 and [S/Fe] = +0.25 respectively. The Zn abundance is derived from two lines at λ4722 Å and λ4810 Å. The value of $\log gf = -0.25$ for the line at λ4810 Å has been obtained from Barbuy et at. (2015). [Zn/Fe] = −0.33 is lower than expected for objects of the thin and thick disk population, i.e., ∼ −0.20 a −0.30 dex (Reddy et al. 2003; 2006). Neutron-capture elements shows [X/Fe] abundances with tendency towards to solar value and ranges from +0.06 to +0.19 dex. Of the elements identified like Y II, Ba II, Ce II and Nd II only the Zr II seems to be found moderately enriched ([Zr/Fe] = +0.45).

5.2. *HD 180028*

HD 180028 is classified as a F6Ib and cataloged as IRAS point source (IRAS 19122 + 0557). The radial velocity were reported by different authors;

TABLE 4

ELEMENTAL ABUNDANCES FOR HD 45674, HD 180028, HD 194951 AND HD 224893.

		HD 45674			HD 180028			HD 194951			HD 224893		
Species	$\log \epsilon_{\odot}$	[X/H]	N	[X/Fe]	[X/H]	N	[X/Fe]	[X/H]	N	[X/Fe]	[X/H]	N	[X/Fe]
C I	8.39	−0.20±0.02	2	−0.36	−0.28±0.10	syn	−0.22	−0.16±0.09	5	−0.01	−0.11±0.10	2	+0.15
N I	7.78	+0.68±0.06	1	+0.52							+0.89±0.06	1	+1.15
O I	8.66	+0.03±0.01	2	−0.13	+0.07±0.10	syn	+0.13	−0.10±0.00	2	+0.05	+0.19±0.05	1	+0.45
Na I	6.17	+0.50±0.10	4	+0.34	+0.37±0.04	2	+0.43	+0.09±0.00	2	+0.24	+0.29±0.04	1	+0.55
Mg I	7.53	+0.08±0.19	4	−0.08	+0.19±0.09	1	+0.25	−0.21±0.09	5	−0.06	−0.34±0.11	3	−0.08
Si I	7.51				+0.19±0.14	3	+0.25	+0.18±0.06	2	+0.33			
Si II	7.51	+0.47±0.13	2	+0.31	+0.06±0.04	1	+0.12				−0.28±0.29	2	−0.02
S I	7.14	+0.41±0.10	5	+0.25	+0.38±0.09	3	+0.44	−0.03±0.10	syn	+0.12			
Ca I	6.31	+0.24±0.11	8	+0.08	+0.07±0.13	5	+0.13	−0.13±0.17	10	+0.02	−0.29±0.03	4	−0.03
Ca II	6.31	+0.16±0.15	2	0.00									
Sc II	3.05	+0.34±0.04	9	+0.18	+0.25±0.09	4	+0.31	−0.03±0.14	6	+0.12	+0.13±0.05	2	+0.39
Ti I	4.90	+0.27±0.10	3	+0.11	+0.15±0.06	1	+0.21	−0.21±0.06	2	−0.06			
Ti II	4.90	+0.29±0.14	14	+0.13	+0.05±0.10	4	+0.11	−0.18±0.12	13	−0.03	−0.20±0.11	13	+0.06
V II	4.00	+0.22±0.02	1	+0.06							−0.24±0.02	1	+0.02
Cr I	5.64	+0.13±0.08	3	−0.03	−0.11±0.10	2	−0.05	−0.34±0.13	5	−0.19	−0.25±0.12	2	+0.01
Cr II	5.64	+0.18±0.12	7	+0.02	−0.11±0.13	3	−0.07	−0.25±0.11	11	−0.10	−0.40±0.09	4	+0.14
Mn I	5.39	+0.14±0.01	3	−0.02	+0.11±0.08	4	+0.17	−0.21±0.18	5	−0.06	−0.21±0.03	1	+0.05
Fe I	7.45	+0.12±0.10	60		−0.06±0.13	56		−0.17±0.11	72		−0.27±0.11	19	
Fe II	7.45	+0.20±0.08	10		−0.06±0.16	8		−0.12±0.11	20		−0.26±0.17	7	
Ni I	6.23	−0.06±0.12	8	−0.22	−0.09±0.06	4	−0.03	+0.10±0.11	6	+0.25			
Ni II	6.23							+0.01±0.04	1	+0.16			
Cu I	4.21				−0.26±0.04	1	−0.20						
Zn I	4.60	−0.17±0.16	2	−0.33	−0.38±0.03	1	−0.32	−0.20±0.10	syn	−0.05	−0.26±0.03	1	0.00
Y II	2.21	+0.11±0.10	5	−0.05	+0.05±0.12	3	+0.11	−0.20±0.15	5	−0.05	−0.20±0.09	4	+0.06
Zr II	2.59	+0.61±0.13	3	+0.45	+0.10±0.04	1	+0.16	−0.12±0.19	2	+0.03			
Ba II	2.17	+0.35±0.07	1	+0.19	+0.23±0.10	syn	+0.29	−0.11±0.07	1	+0.04	−0.34±0.10	2	−0.08
La II	1.13				+0.29±0.05	1	+0.35						
Ce II	1.58	+0.33±0.14	3	+0.17	−0.08±0.16	3	−0.02						
Nd II	1.45	+0.22±0.05	1	+0.06	+0.13±0.09	2	+0.19	−0.11±0.17	2	+0.04			
Eu II	0.52				−0.12±0.10	syn	−0.06						

$-6.0\,\mathrm{km}^{-1}$ (Wilson 1953), $-6.0\,\mathrm{km}^{-1}$ (Duflot et al. 1995) and $-5.1\,\mathrm{km}^{-1}$ (Gontcharov 2006) and does not present variability. Their absorption lines appear slightly wider indicating that rotates with velocity of $23.3\,\mathrm{km}^{-1}$ (De Medeiros et al. 2002).

Their atmospheric parameters were obtained from ionization equilibrium between the lines of Fe I and Fe II reaching values of $T_{\rm eff} = 6400\,\mathrm{K}$, $\log g = 2.1$, $\chi_{\rm t} = 4.8$ and $[\mathrm{Fe/H}] = -0.06$ dex respectively. The surface gravity for HD 180028 was re-affirmed from the equilibrium ionization of other elements such as Si, Ti, Cr, namely $\Delta = [\mathrm{X_{II}/H}]$–$[\mathrm{X_I/H}]$ is 0.11, −0.10 and −0.00 respectively. The atmospheric parameters obtained by different authors and the adopted parameters are found in Table 2.

HD 180028 exhibits a metallicity near to solar of [Fe/H] of−0.06. The abundances of C was obtained by synthesizing the line at 5380 Å reaching values of $[\mathrm{C/H}] = -0.28$ dex and $[\mathrm{C/Fe}] = -0.22$ dex respectively. At temperature of 6100 K the non-LTE correction to C is very small (Takeda 1994) and leads to a value of $[\mathrm{C/Fe}] = -0.39$ dex. In their spectrum are not present N lines or CN bands employee for estimate its abundances. The O abundance was derived by synthesizing the region at 6140–60 Å and where their values are $[\mathrm{O/H}] = +0.07$ dex and $[\mathrm{O/Fe}] = +0.13$ dex respectively (see Figure 3. These values are higher than obtained by Luck (2014). The C/O ratio is about of ∼0.23 which is lower than solar value. From sodium analysis conducted by Andrievsky et al. (2002) found a moderate enrichment of $[\mathrm{Na/Fe}] = +0.28$ dex. The value obtained in this work is slightly higher, i.e. $[\mathrm{Na/Fe}] = +0.43$ dex. The Fe-peak elements show a solar trend. The ratio $[\alpha/\mathrm{Fe}]$ of +0.18 ±0.05 dex seems to indicate that this object belongs to thin disk. Individually, Si, Ca and Ti present solar values while Mg shows a moderate enhancement $[\mathrm{Mg/Fe}] = +0.25$ dex. Sulfur is found be enriched, i.e., $[\mathrm{S/Fe}] = +0.44$ dex. The s-elements show solar-trend except Ba and La which show a modest enhancement.

5.3. *HD 194951*

HD 194951 was classified with F-type by different authors; F2Iab by Stock et al.(1960), F3II by Bidelman (1957) and F1II by Morgan (1972). The physical parameters have been determined by various authors from photometric and spectroscopic techniques (see Table 2) while the values adopted can be seen in the Table 3. The superficial gravity of HD 194951 was re-affirmed from the equilibrium ionization of other elements such as Ti, Cr, and Ni, that is $\Delta = [\mathrm{X_{II}/H}]$–$[\mathrm{X_I/H}]$ is +0.05, +0.09 and −0.09 respectively. The chemical abundances of the elements identified are represented in Table 4.

Carbon abundance is determined from five lines

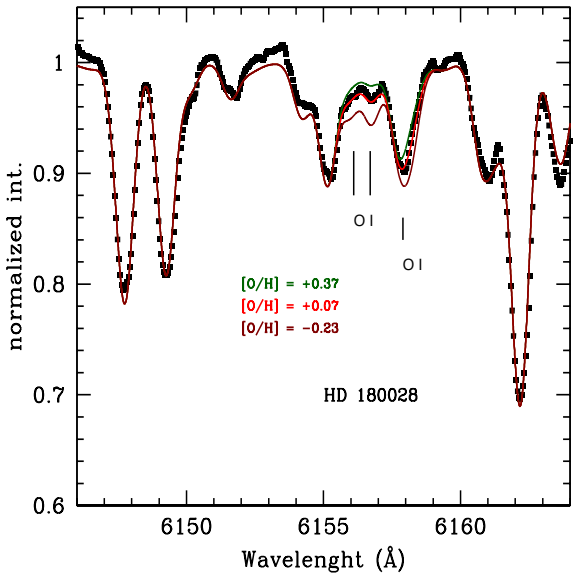

Fig. 3. Observed (filled squares) and synthetic (solid line) spectra of the O I triplet at 6140–60 Å region. The synthetic spectra correspond from top to bottom to [O/H] = =0.37, =0.07 and −0.23 dex respectively.

(λ4769.9 Å, λ4775.8 Å, λ4932.0 Å, λ5380.3 Å and λ6014.8 Å) reaching a [C/H] value of −0.16. At a temperature of 7000 K the non-ETL effects are present and a correction of −0.2 dex for carbon leads to values of [C/H] = −0.36 and [C/Fe] = −0.26 respectively. For O abundance a non-LTE correction of −0.1 dex taken from Takeda & Takada-Hidai (1998) is estimated and the abundances [O/H] = −0.20 and [O/Fe] = −0.10 are near to solar. These C and O abundance values are similar to obtained by Luck (2014). The N line at λ4151.4 Å found for HD 45674 and HD 224893 could not be measured for this spectrum. However, Lyubimkov et al. (2011) were able to study the N abundance for HD 194951 using high-resolution spectra and they found that N is enriched with values of [N/H] = +0.60 and [N/Fe] = +0.73±0.18 respectively.

Our atmospheric model differs in 240 K and 0.12 in effective temperature and surface gravity relative to the model used by Lyumbikov et al., i.e., 6760 K and 1.92. In Table 3 we observe that very few changes in the N abundance appears due to variations of 250 K and 0.5 in T_{eff} and $\log g$. This means we can use this N abundance without being affected by the model. According to the authors the N enrichment has been a general characteristic present in supergiant stars with A and F type that have experienced the first dredge-up (1DUP). The deficiency in C and the enrichment of N indicates that has operated the CN-cycle and the processed material from the H-burning is released on the surface of the star. The C/O = 0.46 ratio is practically solar and it is O-rich star.

The [α/Fe] ratio of +0.06 presents a consistent value for an object belonging to the thin disk population. The Si abundance exhibit a moderate enrichment, i.e., [Si/Fe] = +0.33. Other elements such as Sc, Cr, Mn and Zn shows abundances [X/Fe] between −0.15 up to +0.09 similar to those presented in objects of the thin and thick disk. The Zn abundance is obtained from synthesized line at λ4810.5 Å. [X/Fe] of s-elements range from −0.09 to +0.01, that is, they are on average solar.

5.4. *HD 224893*

Gray et al. (2001b) have determined their atmospheric parameters for this star (see Table 2) and was classified as a bright giant with A8II. Several authors have studied the radial velocity in different epochs, i.e., −22.4 by Adams (1915), −26.4 by Harper (1937), −23.2 by Wilson (1953), −21.9 by Bouigue et al. (1953), −27 by Fehrenbach et al. (1996) and −25.10 km s^{-1} by Gontcharov (2006) respectively, showing very little variations. Danziger & Faber (1972) report a rotation velocity of 40 km s^{-1}.

In this paper is performed for the first time an analysis of abundances in which is included a total of 15 elements. The abundances can be seen in the Table 4. The metallicity of HD 224893 is moderately deficient ([Fe/H] = −0.26 dex). The C abundance is obtained from lines 4770.0 Å and 4771.7 Å respectively. From the LTE analysis we derive a value of [C/H] of −0.11 dex. By taking a non-LTE correction of −0.26 dex (Venn 1995b), either [C/H] and [C/Fe] reaches values of −0.37 dex and −0.19 dex respectively. The N abundance obtained from λ4151.4 Å are [N/H] = +0.89 dex and [N/Fe] = +1.15 dex respectively. The equivalent width of this line is 15.8 mÅ. Under a non-LTE correction of −0.08 dex adopted at 7500K their new values are [N/H] = +0.81 dex and [N/Fe] = +0.99 dex respectively. Like HD 45674 this star shows evidence of having operated CN-cycle and the 1DUP event.

The O abundance is derived from the line at 6158 Å and shows sign of overabundance ([O/Fe] = +0.45), however a non-LTE correction of −0.15 dex at temperature of 7500 K taking from Takeda & Takada-Hidai (1998) leads to values of [O/H] = +0.35 dex and [O/Fe] = +0.53 dex respectively. These values indicate that O abundance show a moderate enrichment. The ratio C/O = 0.26 indicate that HD 224893 is O-rich and has a similar value to HD 45674.

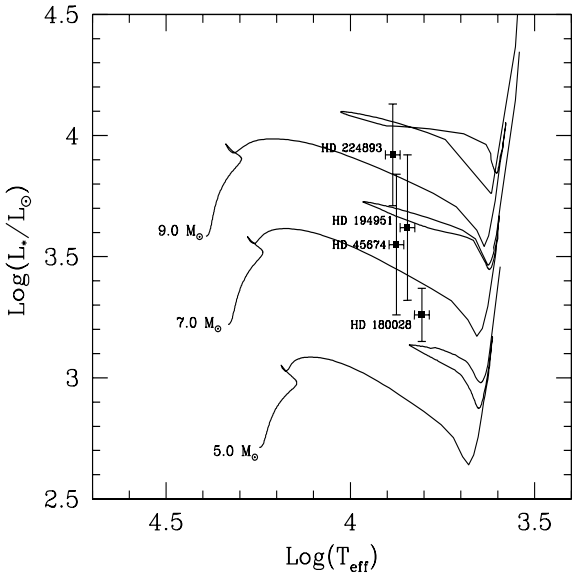

Fig. 4. Locations of HD 45675, HD 180028, HD 194951 and HD 224893 on the HR-diagram. The theoretical evolutionary tracks without rotation with masses of 5, 7 and 9 $M_\odot$ are taken from Ekström et al. (2012) at Z = 0.020.

The abundances [X/Fe] of Fe-peak elements as V, Cr and Mn show solar values except the Sc which has a moderate enrichmenet of +0.39 dex. The alpha-elements ($[\alpha/Fe] = -0.02$ dex), the Zn and the s-elements (Y and Ba) shown sunlike tendencies.

6. DISCUSSION

6.1. *Atmospheric parameters*

The atmospheric parameters taken from literature and those adopted in this work are present in Table 2. We take a mean value of atmospheric parameters of those objects with more than two values. We can note that our adopted values of effective temperature, surface gravity, microturbulence velocity and metallicity are consistent (within the uncertainty limits) with the mean values derived by other authors.

6.2. *Masses*

We also estimated the masses of our sample stars. These can be obtained from their position on the HR-diagram using theoretical evolutionary tracks. We have employed the theoretical evolutionary tracks without rotation with masses of 5, 7 and 9 $M_\odot$ which are taken from Ekström et al. (2012) at solar metallicity (Z = 0.020). Luminosities for HD 45674, HD 194951 and HD 224893 were calculated using $M_V = V_0 + 5 - \log(D)$, where V_0 is the intrinsic colour derived from expresion $V_0 = V - 3.1\,E(B-V)$ and D is the distance estimated from parallaxes (van Leeuwen 2007).

For HD 180028, however, the absolute magnitude have been derived from a mean value ($M_V = -3.38 \pm 0.16$ mag) estimated by Kovtyukh et al. (2012). The bolometric corrections are taken from Masana et al. (2006) and we adopt a solar bolometric magnitude, $M_{Bol} = 4.73 \pm 0.01$ (Gray 2005).

The colour excess for HD 180028, HD 194951 and HD 224893 was obtained using $E(b-y)$ derived from Strömgren photometry by Gray et al. (2001b). We obtain $E(B-V)$ from the relation $E(b-y) = 0.78\ E(B-V)$ (Fernie 1987). For HD 45674 the colour excess is estimated from Schlafly's map (Schlafly & Finkbeiner 2011) and where the dust in the Galactic disc is modelled assuming a thin exponential disc with a scale-height of 125 pc. A correction to colour excess $(B-V)$ have been done for the last assumption. Their values are present at the eleventh column in Table 1.

Figure 4 shows the position of our sample on the HR-diagram. The uncertainty in the luminosity is based in the uncertainties of the parallaxes, visual magnitudes, extinctions and bolometric corrections. Individually, these uncertainties varies like 0.29 (HD 45674), 0.11 (HD 180028), 0.30 (HD 194951) and 0.21 (HD 224893) respectively. According to this position we could to point out that HD 180028 has a mass that vary from 5 to 7 $M_\odot$, HD 45674 and HD 194951 between 7-7.5 $M_\odot$ and HD 224893 of $\sim$9 $M_\odot$.

6.3. *Evolutionary status*

CNO abundances are key to deduce the evolutionary status since their composition reflects the mixing process inside of the stars. These are found summarized in Table 4. With respect to the light elements CNO, we can observe that C abundance for HD 45674, HD 180028, HD 194951 and HD 224893 shows deficiency under non-LTE correction, i.e., these range from -0.04 to -0.69 dex.

For the total sample we were able to identify only one nitrogen line (λ4145.4 Å) for HD 45674 and HD 224893. Their values under NLTE corrections are $[N/Fe] = +0.36 \pm 0.11$ dex and $[N/Fe] = +0.99 \pm 0.14$ dex respectively. Both objects show signs of CN processed material that have been released to the surface. Being unable to estimate the abundance of nitrogen in HD 180028, we can not argue about the eficiency of the CN-cycle on its surface. On the contrary, the N abundance in HD 194951 has been previously studied by Lyubimkov et al. (2011). In fact, Lyubimkov et

al. (2011) found that the nitrogen is enriched, i.e., [N/Fe] = +0.73±0.18 dex.

HD 45674, HD 194951 and HD 224893 show an enhancement of the N abundance. These objects have shown a systematic deficience in the C abundance and a systematic increase in the N abundance indicating the presence of CN-cycle material in stellar surfaces. This enhancement of nitrogen have been also reported previously by Venn (1995b), Venn & Przybilla (2003), Luck & Lambert (1985), Luck & Wepfer (1995) and Smiljanic et al. (2006) in supergiant and bright giant stars.

Three process have been suggested as a result of the surface nitrogen enhancement for massive stars. Consequently, each of case leads to the presence of CN-cycle material in stellar surfaces. In single stars, these process can be due to the severe mass loss, the rotational induced mixing during the MS phase and the dredge-up associated with the deep convective envelope. According to Lyubimkov et al. (2011) the mass loss is one of the process to be unimportant for B-type stars (progenitors of A–F supergiants) within of mass range between 4–15 $M_\odot$. By contrast, the other two process might be found coupled, e.g., it is an observational fact that the mixing process during the 1DUP event might differ between rotating and non-rotating stars. In binary stars, on the contrary, this enhancement is subject to mass transfer of its companion evolved.

In order to verify whether HD 45674, HD 194951 and HD 224893 have already passed through the 1DUP event is necessary to know the [N/C] ratio. The post-1DUP prediction done by Schaller et al. (1992) is approximately [N/C] = +0.60 dex for stars between 2 and 15 $M_\odot$. On the other hand, Meynet & Maeder (2000) calculate evolutionary rotating (with a initial velocity of 300 km s^{-1}) and non-rotating models for masses between 9-120 $M_\odot$. These authors predict [N/C] = +0.72 dex without rotation and [N/C] = +1.15 dex with rotation after the 1DUP and during the blue loop phase for stars with 9 $M_\odot$. For more details see Figure 14 in Smiljanic et al. (2006).

For HD 194951, the [N/C] ratio could be obtained from N abundance derived by Lyubimkov et al. (2011) and C abundance estimated in this work. Here, we must emphasize that our model differs 240 K in T_{eff} and 0.12 in $\log g$ from the model used by Lyubimkov et al. (2011). From Table 3 we can observe that there are small differences of −0.02 (in T_{eff}) and −0.06 (in $\log g$) respectively. These small differences does not affect the N abundance derived by Lyubimkov et al. (2011) due to a change of

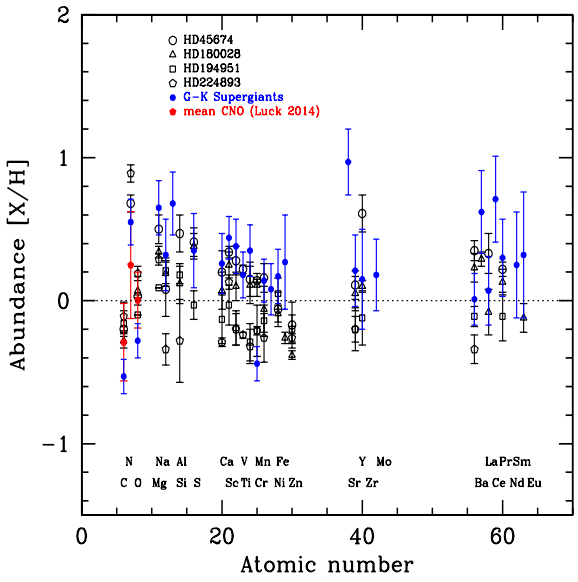

Fig. 5. Comparison of our abundances [X/H] with the mean abundances derived for a sample of G–K young supergiants taken from Luck (1977; 1978) and mean CNO abundances by Luck (2014). Symbols and colour represent data from different sources.

model. Hence, it is possible to use the nitrogen abundance derived by Lyubimkov et al. (2011) with our C abundance. This value is [N/C] = +0.81±0.17 dex. For HD 45674 and HD 224893 we have determined a [N/C] ratio of +0.88±0.09 dex and +1.00±0.13 dex respectively. We note also that these values indicates that both stars show signs of an efficient mixing process. The mean [N/C] ratio for the sample stars is [N/C] = +0.90±0.13 dex.

In short, our results for single and mean [N/C] ratio are larger than the value obtained by Schaller et al. (1992) by a factor between 0.3-0.4 dex and are slightly above of the non-rotating model predicted by Meynet & Maeder (2000), i.e., between +0.72 dex (non-rotating model) and +1.15 dex (rotating model). Our mean value +0.90±0.10 dex would be in agreement with the results for non-rotanting stars with masses of 9 $M_\odot$. Therefore, we may conclude that within of the range of masses that cover our objects (5–9 $M_\odot$) and their [N/C] ratios, HD 45674, HD 194951 and HD 224893 have already experienced the 1DUP event and are in post-1DUP phase. Evolutionarily, the post-1DUP objects can be located only inside the red-blue loop area. Claret (2004) suggests that extensive red-blue loops occur for stars with masses from 6 to 13 $M_\odot$, although this extension is still a matter of controversy (see §6 and Figure 12 in Lyubimkov et al. 2011).

On the other hand, if we consider the effective

temperature and luminosities to be right, the position of HD 45674, HD 194951 and HD 224893 appears to be located within the extended red-blue region with $M =$ 7–9 $M_\odot$ on the HR-diagram. However, the uncertainties causing an appreciable change in the luminosity so that its evolutionary status is unreliable. With regard to HD 180028 if we consider it to have a mass of 5 $M_\odot$ its probable evolutionary status would be located in the red-blue loop region (post-1DUP phase), on the contrary, if we consider it with a mass of 7 $M_\odot$ it appears to be located on the Hertzsprung gap region and moving for the first time towards the red giant/supergiant phase (post-MS phase).

Under non-LTE correction HD 45674, HD 180028, HD 194951 and HD 224893 shows values in O abundance of −0.36, +0.02, −0.10 and +0.53 respectively. HD 224893, by contrast, has a moderate enhancement ([O/Fe] = +0.45) probably due to the CNO bi-cycle. In general, our oxygen values show the observed tendency in objects of the disc studied by Bensby et al. (2014); da Silva et al. (2015).

6.4. *Sodium element*

In our sample we found a moderate enrichment of Na abundances, i.e., [Na/Fe] of +0.34, +0.43, +0.24 and +0.55 derived for HD 45675, HD 180028, HD 194951 and HD 224893 respectively. It is believed that the sodium enrichment is related to the first dredge-up event (Denissenkov & Denissenkova 1990) although this assumption is questioned. The predictions made by models (see Fig. 8 in Karakas & Lattanzio 2014) indicate that the abundance of sodium does not show a significant enrichment in low-mass stars ($M \leq 2\,M_\odot$) from the first dregde-up or by extra-mixing process to solar metallicity (Charbonnel & Lagarde 2010). Even for $M > 2\,M_\odot$ this enrichment does not exceed 0.3 dex.

A non-LTE correction about of −0.10 dex to Na was taken from Lind et al. (2011) and involves values of [Na/Fe] of +0.16, +0.22, +0.24 and +0.37 dex respectively. We noted that our observational results (within their uncertainties) are in agreement with [Na/Fe] predicted by El Eid & Champagne (1995) for intermediate mass stars (∼0.2-0.3 dex).

6.5. *Heavier elements*

The tendency of alpha-elements for our objects is similar to that observed in the thin disk population, i.e., [α/Fe] range from −0.02 to 0.18 dex. The sulfur abundance was estimated synthesizing the spectral region at (6743–6757 Å). [S/Fe] of +0.25 for HD 45675 and +0.12 for HD 194951 shows a similar tendency observed to α-elements of the disc to metallicity near to solar value (Caffau et al. 2005). By contrast, S abundance for HD 180028 is overabundant, i.e., [S/Fe] = +0.44 dex. Iron-peaks and neutron-capture elements in all sample stars show [X/Fe] abundances with tendency towards to solar value. HD 45674 and HD 180028 shows a modest enrichment of Zr II and La II of +0.45 dex and +0.32 dex respectively.

6.6. *Comparison with other supergiants*

Our [X/H] abundances can be compared with the mean abundances derived from a sample of G–K young supergiant stars studied by Luck (1977; 1978) and mean CNO abundances by Luck (2014). Figure 5 shows the [X/H] abundances versus atomic number. The abundances in the sample stars of the present paper are shown with different symbols together with their uncertainties, i.e., HD 45674 (open circle), HD 180028 (open triangle), HD 194951 (open square) and HD 224893 (open pentagon), the cool supergiants are represented with a blue filled circle and CNO abundances with red filled pentagon respectively. We can see, in general, that abundances of our sample stars (e.g., CNO, α, Fe-peak and neutron capture elements) follow the trends expected from Galactic chemical evolution of the Population I.

7. CONCLUSIONS

From this study we performed a detailed analysis of the photospheric abundances for a sample of four A–F type supergiant stars of intermediate mass (∼5–9 $M_\odot$) using high-resolution spectra. We have determined atmospheric parameters, masses and abundances using spectral synthesis and equivalent widths. Our three stars (HD 45674, HD 194951 and HD 224893) for which we were able to determine both carbon and nitrogen show signs of internal mixing. A mean [N/C] ratio of +0.90±0.13 dex is found and this value is in agreement with the preditions of non-rotating models by Meynet & Maeder (2000), which predict [N/C] =+0.72 dex. A surface nitrogen enhancement was observed in these stars and it only could comes from as a result of deep mixing during the 1DUP. The sample of three stars shows very little variability in radial velocities by discarding binarity in them.

According to abundances analysis we can conclude that HD 45674, HD 194951 and HD 224893 show typical values of abundances for supergiants of the thin disc population and where evolutionarily the post-first dregde-up (post-1DUP) phase was

reached. These objects are located in the red-blue loop region. HD 180028, on the contrary, also show typical abundances of the population I but its evolutionary status could not be satisfactorily defined.

Acknowledgments

This work has made extensive use of ELODIE, SIMBAD and ADS-NASA database to which we are thankful. The authors thanks an anonymous referee for fruitful comments and suggestions to improve this work.

REFERENCES

Adams W.S., 1915, ApJ, 42, 172
Andrievsky S.M., Egorova I.A., Korotin S.A., Burnage R., 2002, A&A, 389, 519
Asplund M., Grevesse N., Sauval A.J., 2005, ASPC, 336, 25
Barbuy B., Friaca, A.C.S., da Silveira C.R., Hill V., Zoccali M., Minniti D., Renzini A., Ortolani S., Gómez A., 2015, A&A, 580, 40
Bensby T., Feltzing S., Oey M.S., 2014, A&A, 562, 71
Bidelman W.P., 1957, PASP, 69, 326
Bidelman W.P., 1993, ASPC, 45, 49
Bouigue R., Chapuis J.L., 1953, Publ. Obs. Haute-Provence, 2, 50
Caffau E., Bonifacio P., Faraggiana R., Francois P., Gratton R.G., Barbieri M., 2005, A&A, 441, 533
Castelli F., Kurucz R.L. 2003, Modelling of Stellar Atmospheres, Poster Contributions. Proceedings of the 210th Symposium of the International Astronomical Union held at Uppsala University, Uppsala, Sweden, 17-21 June, 2002. Edited by N. Piskunov, W.W. Weiss, and D.F. Gray. Published on behalf of the IAU by the Astronomical Society of the Pacific, 2003., p.A20
Charbonnel C., Lagarde N., 2010, A&A, 522, 10
Claret A., 2004, A&A, 424, 919
Da Silva R., Milone A.C., Rocha-Pinto H., 2015, A&A, 580, 24
Danziger I.J., Faber S.M., 1972, A&A, 18, 428
De Medeiros J.R., Udry S., Burky G., Mayor M., 2002, A&A, 395, 97
Denissekov P.A., Denissenkova S.N., 1990, Soviet Astronomy Letters, 16, 275
Duflot M., Figon P., Meyssonnier N., 1995, Baltic Astronomy, 5, 83
Ekström S., Gorgy C., Eggenberger P., et al., 2012, A&A, 537, A146
El Eid M.F., Champagne A.E., 1995, ApJ, 451, 298
Fehrenbach C., Duflot M., Genty V., Amieux G., 1996, Bull. Inf. Centre Donnees Stellaires, 48, 11
Fernie J.D., 1987, AJ, 94, 1003
Fürh J.R., Wiese W.L., 2006, J. Phys. Chemical Reference Data 35, 1669
Gray D.F., 2005, The Observation and Analysis of Stellar Photospheres (Cambridge: CUP), p. 506
Gray R.O., Graham P.W., Hoyt S.R., 2001b, AJ, 121, 2159
Gontcharov G.A., 2006, Astron.Lett., 32, 759
Harper W.E., 1937, Publ. Dominion Astrophys. Obs., 7, 1
Hohle M. M., Neuhäuser R., Schutz B. F., 2010, AN, 331, 349
Karakas A.I., Lattanzio J.C., 2014, PASA, 31, 30
Kaufer A., Venn K.A., Tolstoy E., Pinte C., Kudritzki R.P., 2004, AJ, 127, 2723
Kurucz R.L., Furenlid I., Brault J., Testerman L., 1984, National Solar Observatory Atlas. National Solar Observatory, Sunspot, New Mexico
Kovtyukh V.V., 2007, MNRAS, 378, 617
Kovtyukh V.V., Gorlova N.I., Belik S.I., 2012, MNRAS, 423, 3268
Lind K., Asplund M., Barklem P.S., Belyaev A.K., 2011, A&A, 528, 103
Luck R.E., 1977, ApJ, 218, 752
Luck R.E., 1978, ApJ, 219, 148
Luck R.E., 2014, AJ, 147, 137
Luck R.E., Lambert D.L., 1985, BAAS, 17, 560
Luck R.E., Lambert D.L., 1985, ApJ, 298, 782
Luck R.E., Moffett T.J., Barnes III T.G., Gieren W., 1998, AJ, 115, 605
Luck R.E., Wepfer G.G., 1995, AJ, 110, 2425
Lyubimkov L.S., Lambert D.L., Korotin S.A., Poklad D.B., Rachkovskaya T.M., Rostopchin S.I., 2011, MNRAS, 410, 1774
Masana E., Jordi C., Ribas I., 2006, A&A, 450, 735
Mélendez J., Barbuy B., 2009, A&A, 497, 611
Meynet G., Maeder A., 2000, A&A, 361, 101
Morgan W.W., 1972, AJ, 77, 35
Moultaka J., Ilovaisky S.A., Prugniel Ph., Soubiran C., 2001, PASP, 116, 693
Prugniel P., Soubiran C., 2001, A&A, 369, 1048
Prugniel P., Soubiran C., Koleva M., Le Borgne, D., 2007, ELODIE library V3.1, VizieR On-line Data Catalog: III/251. Originally published in: astro-ph/0703658
Przybilla N., Butler K., 2001, A&A, 379, 955
Reddy B.E., Lambert D.L., Allende Prieto C., 2006, MNRAS, 367, 1329
Reddy B.E., Tomkin J., Lambert D.L., Allende Prieto C., 2003, MNRAS, 340, 304
Schaller G., Schaerer D., Meynet G., Maeder M., 1992, A&AS, 96, 269
Schlafly E.F., Finkbeiner D.P., 2011, ApJ, 737, 1035
Smiljanic R., Barbuy B., De Medeiros J.R., Maeder A., 2006, A&A, 449, 655
Sneden C. 1973, PhD. Thesis, Austin-Texas
Soubiran C., Le Campion J.F., Cayrel de Strobel G., Caillo A., 2010, A&A, 515, 111
Stock J., Nassau J.J., Stephenson C.B., 1960, Hamburger Sternw., Warney & Swasey Obs., 2, 0
Stothers R.B., Chin C.W., 1991, ApJ, 381, 67
Stothers R.B., Chin C.W., 1976, ApJ, 204, 472
Sumangala Rao S., Giridhar S., Lambert D.L., 2012, MNRAS, 419, 1254

Takeda Y., 1994, PASJ, 46, 53
Takeda Y., Takada-Hidai M., 1998, PASP, 50, 629
Van Leeuwen F., 2007, A&A, 474, 653
Venn A.K., 1995a, ApJS, 99, 659
Venn A.K., 1995b, ApJ, 449, 839
Venn A.K., Lennon D.J., Kaufer A., et al., 2001, ApJ, 547,765
Venn A.K., Mc Carthy J.K., Lennon D.J., Przybila N., Kudritzki R.P., Lemke M., 2000, ApJ, 541, 610
Venn A.K., Tolstoy E., Kaufer A. et al., 2003, AJ, 126, 1326
Venn A.K., Przybilla N., 2003, CNO in the Universe, ASP Conference Series, Vol. 304
Walmswell J.J., Tout C.A., Eldridge J.J., 2015, MNRAS, 447, 2951
Wilson R.E., 1953, Carnegie Ins. Washington D.C. Publ., 601, 0
Wu Y., Singh H.P., Prugniel P., Gupta R., Koleva M., 2011, A&AS, 525, 71

R. E. Molina: Laboratorio de Investigación en Física Aplicada y Computacional, Universidad Nacional Experimental del Táchira, Venezuela, (rmolina@unet.edu.ve).
H. Rivera: Laboratorio de Investigación en Física Aplicada y Computacional, Universidad Nacional Experimental del Táchira, Venezuela, (hrivera@unet.edu.ve).